Ocean Sci. Discuss., 10, 985–1030, 2013
www.ocean-sci-discuss.net/10/985/2013/
doi:10.5194/osd-10-985-2013

Ocean Science
Discussions
Open Access

Frontal structures in the West Spitsbergen Current margins

W. Walczowski

Institute of Oceanology Polish Academy of Sciences, Powstancow Warszawy 55 81-712 Sopot, Poland

Received: 14 May 2013 – Accepted: 14 June 2013 – Published: 2 July 2013

Correspondence to: W. Walczowski (walczows@iopan.gda.pl)

Published by Copernicus Publications on behalf of the European Geosciences Union.

Abstract

The structures of the hydrographic fronts separating the Atlantic origin waters from ambient waters in the northern Nordic Seas are discussed. Flows of the western and eastern branches of the West Spitsbergen Current create the Atlantic domain borders and maintain these fronts. The work is based on previous research and on investigations in the project DAMOCLES (Developing Arctic Modeling and Observational Capabilities for Long-term Environmental Studies). Most of the observational data were collected during the R/V *Oceania* cruises. The main focus of the paper is put on the western border of the Atlantic domain – the Arctic Front, along- and transfrontal transports, the front instability and variability. The baroclinic instability and advection of baroclinic eddies which occurs due to this instability were found as the main transfrontal transport processes. Most of the Atlantic Water transported by the western branch recirculates west and southward. The eastern branch of the West Spitsbergen Current provides most of the Atlantic Water entering the Arctic Ocean. Both processes are very important for the Arctic and global Thermohaline Circulation.

1 Introduction

Most of the Atlantic Water (AW) that enters the Nordic Seas (Norwegian, Greenland, and Iceland Sea) flows over the Faroe-Iceland Ridge and between the Faroe and Shetland Islands (Hansen and Osterhus, 2000). There are two main branches of the AW inflow east of Iceland. The colder, less saline western branch (the Faroe Branch) of the Norwegian Atlantic Current is topographically guided from the Iceland-Faroe Front towards the Fram Strait (Fig. 1). In the Nordic Seas it acts as the jet of the Polar Front (Orvik and Niiler, 2002). The warmer, more saline eastern branch of the AW (the Shetland Branch) enters the Nordic Seas through the Faroe-Shetland Channel and continues north along the Norwegian shelf edge as the Norwegian Atlantic Slope Current (NASC) (Orvik and Skagseth, 2003). After passing the northern Norway, the NASC

OSD
10, 985–1030, 2013

branches. One stream of the AW enters the Barents Sea as the North Cape Current (the Barents Sea Branch) and flows into the Arctic Ocean (AO), mostly through the St. Anna Trough (Schauer et al., 2002; Maslowski et al., 2004). The second branch continuing north along the continental slope is called the West Spitsbergen Current (WSC) (Aagaard and Carmack, 1989). Nowadays this flow is often called the WSC eastern branch or the core of the WSC; correspondingly, the continuation of the Faroe Branch linked with the oceanic frontal system is called the WSC western branch. These two currents and hydrological fronts related to the both branches of the WSC create dynamic borders of the region occupied by the AW – the Atlantic domain (AD) of the Nordic Seas (Fig. 1). There is a large scale oceanic front in the west, and shallow water, local scale front in the east. Both fronts separate the Atlantic-origin waters from the ambient, much colder and fresher water masses.

In the Nordic Seas the Meridional Overturning Circulation (MOC) becomes more of a horizontal loop. The warm, buoyant waters flow northward in the east, the cold, dense waters flow towards the Atlantic in the west (Mauritzen, 2011). This two way oceanic exchange that connects the Arctic and Atlantic oceans are of fundamental importance to climate (Dickson et al., 2008). The importance of the fronts – flexible borders between warm and cold water masses is related to the importance of the whole Nordic Seas for the global climate.

Fronts create the barrier between waters of different properties and origin. There are strong horizontal gradients of all properties across the front. Contact of water masses of various densities generates alongfrontal baroclinic jet streams, which keeps the front in the dynamic equilibrium state (Fedorov, 1986). This frontal barrier is not solid – frontal zone changes its position, water mixes and exchanges across the front. In the case of the Atlantic domain in the Greenland Sea, processes of transfrontal exchange, especially through the western border are very important; it is the vital part of the northern limb of the Atlantic Meridional Overturning Circulation (AMOC). Water masses formed in the Nordic Seas and the Arctic Ocean supply the Greenland-Scotland Ridge

OSD
10, 985–1030, 2013

overflow and maintain the lower limb of the Atlantic Meridional Overturning Circulation (Kuhlbrodt et al., 2007).

Existence of the intensive northward current over the Mohn and Knipovich Ridges has been postulated for a long time (Dietrich et al., 1980). Old maps of Alekseev and Isothin from 1955 showed 3 branches of the Norwegian Atlantic Current, in Wegner's map from 1963 splits of the North Atlantic Current into 2 branches of the Norwegian Current at the latitude of southern Norway occurs. Both branches re-join west of Svalbard (Fig. 2). Also, the Institute of Oceanology, Polish Academy of Sciences (IOPAN) works (Piechura and Walczowski, 1995; Walczowski, 1997) suggested existence of the second WSC branch formed by the baroclinic alongfrontal jet streams.

For a long time the role of these flows was not appreciated. The common mistake made by all authors was claiming that both NAC branches originate from only one AW inflow through the Faroe-Shetland Channel. Monitoring the Faroe Branch (Hansen et al., 1999) of Atlantic inflow over the Greenland-Scotland Ridge in late 90s helped understand the AW pathways in the Nordic Seas.

In this work the frontal structures bordering the northern part of the AD and several processes occurring there are described. The additional aim of this study is to quantify the importance of the hydrographic fronts separating the Atlantic Waters in the Nordic Seas from other water masses. The used data sets and applied methods are introduced in Sect. 2. In Sect. 3, the structure of the AD is described. Section 4 provides a description of the western AD border, and Sect. 5 refers to the eastern AD border. Section 6 summarizes the main conclusions of the present study.

2 Data and methods

Every summer since 1987, the IOPAN research vessel *Oceania* operates in the region between the northern Norway and the Fram Strait. The main objectives of this work include investigation of the AW flow through the Norwegian and Greenland Seas, water properties and modification. During the R/V *Oceania* cruises vertical profiles along

OSD
10, 985–1030, 2013

standard sections (Fig. 3) are performed. The zonal sections are perpendicular to the general direction of the AW advection. Two meridional sections close the AW inflow into the Barents Sea. IOPAN's main efforts focus on the northern part of the AD, where processes controlling the AW inflow into the Arctic Ocean through the Fram Strait and westward recirculation take place. Herein the part of the Atlantic domain between the latitudes of 74° N and 79° N is described.

The same station grid was used during the EU project DAMOCLES (Developing Arctic Modeling and Observing Capabilities for Long-term Environmental Studies). During 4 yr of the project more than 800 station were taken. All observations were carried out in summer and the gathered data allow only for the summer-to-summer variability analysis.

The equipment used for measurements include Seabird CTD (SBE 911+) with duplicate temperature and conductivity sensors (since 2008) and the Lowered Acoustic Doppler Current Profiler (LADCP) (since 2005). Every year the temperature and conductivity sensors are calibrated by the Sea-Bird Electronics service.

The data from the same sections covered by the measurements in summers 2000–2010 were used. Mean water properties were calculated from gridded fields. Data were interpolated using optimal interpolation methods, the kriging procedures (Emery and Thomson, 2001). The rectangular grids were smoothed with a linear convolution low-pass filter. Furthermore, the Ocean Data View software with the Data-Interpolating Variational Analysis (Troupin et al., 2012) gridding procedures was used. Baroclinic currents across sections were calculated with reference to the bottom (i.e. taking zero current at the bottom irrespective of depth). For horizontal distributions, currents were calculated with reference to 1000 dbar. The current vectors indicate only the baroclinic component of the flow, but offer a good representation of the general pattern of the flow (Walczowski et al., 2005). The heat content was calculated with respect to a temperature of −0.1 °C.

For the years 2005–2010, CTD data from the Norwegian Gimsøy Section, provided by the Institute of Marine Research, Bergen, were also used. Additionally, in order

OSD
10, 985–1030, 2013

to provide an explanation of the frontal mesoscale structures, data from the process-oriented experiments performed by IOPAN in summers 1995 and 1996 were used.

LADCP data were applied as well. The downward-looking LADCP was attached to the CTD rosette. The results were processed with the LDEO IX software for Matlab (Thurnherr, 2007).

There are several water mass characteristics in the Nordic Seas. Herein the AW was defined as warmer than 0 °C and saltier than 34.92. In practice, in the majority of casts, both the upper and lower limits of the analysed water column were determined by salinity, and the mean properties of the AW layer were calculated for the water column satisfying the condition $S \geq 34.92$. For comparison with other works, characterization of the AW as water warmer than 2 °C and more saline than 34.90 was also applied.

3 The Atlantic domain structure and currents pattern

The shape of the Atlantic domain is strongly related to the bottom topography. In the west, the mid-ocean ridges system of the Mohn Ridge and the Knipovich Ridge creates a natural barrier separating the Atlantic and Arctic waters. Located between latitudes 70°–73° N, the Mohn Ridge stretches towards the north-east. The northern extension of the Mohn Ridge – the Knipovich Ridge stretches north towards the Fram Strait. At a depth of ca. 2500 m, the ridge rises 250–500 m above the bottom. There are also several high submarine mountains, elevating even 2000 m over the bottom level. On the western side of the ridge, there is a trench of a depth of several hundred meters; the Arctic domain is deeper than the Atlantic one.

The eastern border of the AD is limited by shallow waters. South of the 74° N parallel, between the North Cap and the Bear Island, a part of the AW advects eastward through the Barents Sea Opening – a trench in the Barents Sea slope of a depth of ca. 480 m. North of the 74° N parallel the eastern AW boundary is formed by the Barents Sea and the western Spitsbergen slopes and shelves.

OSD
10, 985–1030, 2013

Along the AD borders, two branches of the WSC continue. The eastern branch continues as an intensive, narrow flow with core over the 800 m isobath. The AW temperature and salinity reach the maximum in these stream. Eastward tilt and deepening of the θ, S, and δ_θ isolines (Fig. 4a–c) indicate existence of the northward current's baroclinic component; baroclinic velocities exceed 25 cm s^{-1} (Fig. 4d). The AW occupies also the outer part of the shelf where the local front between the AW and the Polar Water exists. The western branch, continuing over the ridges, is maintained by the baroclinic frontal jet streams. The baroclinic front is manifested by outcrop of all isolines (Fig. 4). In this branch the northward stream is wide, less concentrated than that in the eastern side, nevertheless, the baroclinic component of the northward flow reaches 40–50 cm s^{-1}.

Changes of the bottom topography and convergence of isobaths in the northern part causes confluence of both WSC streams at 78° N and narrowing of the AD (Walczowski et al., 2005). Continuing north of the 78° N parallel, the streams diverge and divide into paths which inflow the AO or recirculate westward (Fig. 1). Correspondingly to the shape of the borders, the AD forms a wedge which is wide in the southern part and narrow in the north (Fig. 3). The width of the AD in the south, near the Bear Island latitude, amounts to 350–400 km, whereas in the vicinity of the Fram Strait, the width decreases to 100 km. Depending on the region and the AW definition, thickness of the AW layer reaches 800–1000 m (Fig. 4). The vertical gradients of properties (thermocline, halocline, pycnocline) separate the AW layer from intermediate waters (Fig. 5).

The AW flow between main streams is slower and follows in both directions. The mesoscale activity with mostly anticyclonic eddies is intensive. Numerous flow reversals in the central part result in a comparatively small volume transports, considering the large areas covered by the AW. This causes small average northward velocities in the Atlantic domain despite the relatively high local speeds (Cisewski et al., 2003). Indeed, the mean signal propagation velocities are estimated between 2 cm s^{-1} and 4 cm s^{-1}. (Furevik, 2000; Cisewski et al., 2003; Walczowski and Piechura, 2007).

OSD
10, 985–1030, 2013

West of the AF the Return Atlantic Water (RAW) occurs. This water mass originates from the AW recirculated in the Fram Strait and the Arctic Ocean or transported across the AF. The salinity, temperature and thickness of the RAW is lower than the AW on the east side of the front, the RAW frequently forms mesoscale, anticyclonic eddies.

4 The western boundary of the AD

4.1 Structure of the Arctic Front

Between the Polar domain occupied by the water carried directly from the AO by the East Greenland Current and Atlantic domain, there is a region called the Arctic domain. This domain, containing the cyclonic Greenland Sea Gyre, is bounded by large-scale climatological fronts. On the east the front is formed by the confluence of the Arctic and the Atlantic origin water masses. There are various names for this structure: the Polar Front (Orvik and Niiler, 2002), the Polar Ocean Front (Johannessen, 1986), the Arctic Frontal Zone (van Aken et al., 1995). Herein, we call it, after Swift (1986), the Arctic Front (AF), to distinguish between this front and the border between the Polar and Arctic waters, called the Polar Front. This term may be also confusing, because the term "Arctic Front" is sometimes used for the local front which bounds the Atlantic domain on the east side (Soloranta and Svendsen, 2001).

The AF is an 800 km long and 40–80 km wide zone of strong horizontal and vertical gradients of all properties. Baroclinic jet streams maintain flows on both sides of the front. Some authors (Van Aken et al., 1995) define the AF as the multifrontal zone with cold Greenland Sea Gyre in the west, the AW jet streams in the east and a band of mesoscale eddies in between. From the south the front is a continuation of the Iceland-Faroe Front; in the north the front bifurcates in the Fram Strait region. Horizontal dimensions of the AF are compared with geophysical scales and the front can be classified as a macroscale climatic phenomenon (Fedorov, 1986).

OSD
10, 985–1030, 2013

In the Nordic Seas circulation tends to follow f/H contours (Hopkins, 1991). Also the AF is strongly related to the bottom topography. This indicates that the large-scale deformation field responsible for the frontogenesis has to be of a barotropic nature (Spall, 1997). The ADCP and LADCP measurements confirm existence of the barotropic component of flow in the WSC (Osinski et al., 2003; Walczowski et al., 2005). In the western branch the barotropic currents reach up to 5 cm s^{-1}.

The deformation field causes stretching of isolines and overlaying of lighter AW above denser waters from the Greenland Sea Gyre. Isothermal, isohaline and isopycnic surfaces slope down from the upper layers on its cold Arctic side to intermediate depths on the Atlantic side (Fig. 4). Angle of the slope is about 1°, the largest inclines exceed 1.6°. Below the AW cover, the intermediate and deep waters are disposed. The Arctic Waters are cold, less saline and denser.

Horizontal gradients of all properties occur under the surface mixed layer at the level of 100–700 dbar. Maximal horizontal gradients occur at 200–300 dbar but even here they are rather small in comparison with other climatic fronts (Fedorov, 1986). For the AF the typical temperature horizontal gradient remains at the value of 0.30–0.40 °C km^{-1}, the salinity gradient is 0.02–0.03 km^{-1} and the density gradient is 0.015 kg m^{-3} km^{-1}. The weak horizontal density gradient may be one of the reasons for frontal instability and meandering (Ivanov and Koroblev, 1994).

In summer 2009, at the latitude of 76°30′ N, at the level of 200 dbar, the temperature between the Arctic and Atlantic sides varied from 0 °C to 3.8 °C, salinity varied from 34.90 to 35.09 and potential density from 27.91 to 28.03 kg m^{-3} (Fig. 5). It makes horizontal gradients of temperature equal to 0.25 °C km^{-1}, salinity 0.013 km^{-1} and density 0,014 kg m^{-3} km^{-1}. There is a positive correlation between the temperature and salinity fields: increasing of water temperature is linked with increasing of salinity. The horizontal density gradient is due to differences of temperature between the Arctic and Atlantic waters; changes in salinity across the front partly compensate temperature effect and weaken the density gradient.

OSD
10, 985–1030, 2013

In the AW column, salinity inversion occurs – salinity decreases with depth. Stability of the water column is caused by the temperature vertical gradient. It is possible due to large value of density ratio R_ρ, which is defined as:

$$R_\rho = \frac{\alpha \frac{\partial \theta}{\partial z}}{\beta \frac{\partial S}{\partial z}} \tag{1}$$

where the thermal expansion coefficient α and saline contraction coefficient β are defined by:

$$\alpha = -\frac{1}{\rho}\left(\frac{\partial \rho}{\partial \theta}\right)_{p,S} \tag{2}$$

$$\beta = \frac{1}{\rho}\left(\frac{\partial \rho}{\partial S}\right)_{p,\theta} \tag{3}$$

Despite the fact that the salinity inversion does not occur in the Arctic domain, vertical stability of the Arctic Water column is lower than in the Atlantic domain.

4.2 The AF dynamics

The Rossby Number:

$$Ro = \frac{\overline{v}}{f \cdot L} \tag{4}$$

where L is the horizontal length scale and f is the Coriolis parameter defined by:

$$f = 2 \cdot \Omega \cdot \sin(\varphi) \tag{5}$$

estimated for width of the front $L = 80\,\mathrm{km}$, mean current velocity $= 25\,\mathrm{cm\,s^{-1}}$ and the Coriolis parameter for the latitude of 75° N, $f = 1.37\ 10^{-4}\,\mathrm{s^{-1}}$, equals 0.23 and fulfils the

OSD
10, 985–1030, 2013

condition for macroscale flows: $Ro \ll 1$ (Druet, 1994). It means that the front is in quasi-geostrophic balance and that geostrophic approximation may be applied. Besides the baroclinic pressure, the Coriolis force is the main factor which influences the dynamics of the front. Ageostrophic flows are very weak (Gill, 1982) but may play a significant role in transport across the front.

The core of the AW flow is located in the zone of the steepest front slope (Fig. 4d). The maximal velocity of baroclinic jets reaches 50 cm s^{-1}. The jet often splits into two streams. The width of the streams reaches about 40 km. Considerable summer to summer variability of the flow field is apparent (Fig. 6); it concerns the field structure, the location of the main stream and its properties.

For data collected by IOPAN in summers 1996–2010 the mean geostrophic AW volume and heat transport at the latitude of 76°30′ N for the 65 km wide zone between the longitudes 6°30′ E (65th km in Fig. 4) and 9° E (130th km in Fig. 4) equalled, respectively, 1.5 Sv and 18.5 TW with standard deviations of 0.9 Sv and 12.3 TW, respectively. It changes considerably over time (Fig. 7). The maximal transports in summer 2004 exceed 3 Sv of volume and 40 TW of heat carried with the AW ($S > 34.92$, $T > 0$). Changes of the heat transport are caused by changes in the volume transport; differences of the AW temperature play minor role.

4.3 The mesoscale activity within the AF

Flow instabilities may take a variety of forms, and the mechanisms are often difficult to identify observationally (Gill, 1982). Stratification of the water mass, structure of the flow, horizontal and vertical properties gradients are factors which affect the front stability. During the AF study, a few mesoscale features, such as meanders and eddies, were found. The size of the eddies were in the order of the Rossby deformation radius, which in these region reaches 9–11 km. Presence of meanders and eddies indicate that the AF is sensitive to instability and suggests that a large-scale deformation field is active and frontogenesis processes take place. The kinetic energy of barotropic motion

OSD
10, 985–1030, 2013

is converted into the potential energy of stratified water by elevating particles above the level specific for their density, which causes sloping of the isopycnic surfaces.

The energy which is possible to extract, the Available Potential Energy (APE), is described as (Gill, 1982):

$$\mathrm{APE} = \int\int \frac{1}{2}\rho g \eta^2 \mathrm{d}x\mathrm{d}y \tag{6}$$

where η means particle elevation. The transformation of energy from the vertical stratification into the mesoscale circulation occurs in the baroclinic instability process. Water particles moving down along the inclined isopycnic surfaces convert their potential energy into the kinetic one. It is possible in regions of strong baroclinicity, i.e. where significant baroclinic currents occur, and the vertical shear of the current exists. In the state of geostrophic equilibrium only a small part of the APE may be converted into kinetic energy; rotation prevents the energy transformation.

Mesoscale eddies may be also created in the barotropic instability mechanism. By the horizontal shear of the flow, eddies gain energy directly from the mean flow's kinetic energy.

In case of the AF, maximal values of the horizontal velocity gradient $\partial v/\partial x$ are 1 to 2 orders less than the vertical velocity gradients. This suggests that the possibility of barotropic instability occurrence is much less than the baroclinic instability. The Burger number:

$$S = \left(\frac{R_\mathrm{D}}{L}\right)^2 \tag{7}$$

calculated for the width of the front as it is in a geostrophic equilibrium state $L = 80$ km and the Rossby radius of deformation $R_\mathrm{D} = 10$ km, equals 0.016. This also indicates that only a small part of the energy needed for front destabilisation is gained from barotropic instability, and disturbances are created mainly due to the APE releasing via baroclinic instability processes (Druet, 1994).

OSD
10, 985–1030, 2013

One of the aims of the process-oriented observation conducted in 1995 and 1996 within the AF was to investigate the processes of the frontal instability development. In 1995, the horizontal and vertical tracers distributions indicated the presence of two – anticyclonic and cyclonic – meanders in different stages of development (Fig. 8). The sections along the 74° N parallel (Fig. 9) showed that the front and the main AW flow was situated on the eastern side and was associated with cyclonic circulation. Calculations shows (Walczowski, 1998) that only 30 % of the water flowed along the anticyclonic meander, a temporarily existing structure created as a result of the front destabilisation. This warm, salty core meander was in a transformational phase on its way to becoming an eddy. The radius of the meander was about 40 km. In the centre of the meander water circulated along closed orbits. The period of circulation, which was calculated, was about 120 h. The maximum radius of the eddy exceeded 20 km, which is twice that of the Rossby radius of deformation. The eddy depth reached 450 m. The meander was connected with the main front only from the surface layer to 150 m. At deeper levels the front and the meander are visible as separate structures.

Also in 1996 a system of eddies and meanders was found (Fig. 10). The warm salty anticyclonic meander (with its centre at 74°20′ N, 7°45′ E) was an unstable, nearly separated, "young" elliptical eddy. The horizontal and vertical dimensions of the eddy were bigger than those of the eddy found in 1995, maximal radius was 33 km. The eddy reached 650 m in depth, but its horizontal temperature gradients were visible even at the 800 dbar level.

Two years of investigations did not provide a clear answer regarding the causes of front meandering and eddy creation. These processes are complicated and the interaction of different factors take place. Investigations of the frontal dynamic suggest that the instability of fronts and eddy creation is a mechanism which limits frontogenesis provided by the deformation field (Spall, 1997). In this context, the presence of eddies indicates deformation field activity. The intensity of eddy creation may be a measure of frontogenesis process strength. Front meandering, a growth and the expansion of meanders are possible due to the release of the APE and its transformation into ki-

OSD
10, 985–1030, 2013

netic energy. Unstable meanders can produce eddies. Warm, salt meanders produce anticyclonic eddies which migrate to the Arctic domain carrying salt and heat.

Also the bottom topography plays a significant role in the eddies creation process. Occurrence of the underwater mountains supports the eddies creation. The meandering of the front over the Schultz Bank – underwater mountain at 73°50′ N, 7°30′ E has been observed for a few times (Walczowski, 1997).

Thermohaline intrusions (Fig. 11) are another important phenomenon often observed along the AF. The occurrences of low-saline cold intrusions advecting from the Arctic towards the Atlantic domain have been frequent. Warm, saline intrusions were less distinct, probably because of their tendency to move upward (Hallock, 1985) towards the mixed layer. The observed intrusions were even 40 km long and 100 m thick. The role of this phenomenon in the frontal system ranges widely from frontolysis processes to the transfrontal transport of heat, salt and volume. The sinking of cold intrusions may be an efficient mechanism of the APE release and the cause of baroclinic instability. Intrusion closed inside baroclinic eddies should help in eddy dissipation.

4.4 Cross-frontal eddy transport

The location of the AF in the AMOC northern limb determines the significance of both alongfrontal and transfrontal transport processes. Preconditioning to deep water formation, which is possible due to salt transport towards the Greenland Sea, makes the transport of the AW towards the Greenland Sea gyre especially important. This transport is also necessary to close the heat and freshwater budget of the Greenland Sea (Latarius and Quadfasel, 2010; Segtnan et al., 2011).

The cross-frontal transport was calculated by Walczowski (1998). The anticyclonic eddies were recognised as the main mechanism of the transfrontal transport. Salt, heat fluxes and transport were estimated from field data by calculating the mean salt and heat carried by an eddy and estimating the eddies generation rate. To calculate the amount of salt carried by a single eddy, approximations have to be made using Gaussian curves of salinity anomaly at specific isobaric levels. A similar method, with

OSD
10, 985–1030, 2013

the exception of isopycnic surfaces, was used for the Iceland-Faeroes Front (Allen et al., 1994). The method was also used to calculate the temperature anomaly and heat transport by the eddy (Walczowski, 1997).

Based on the field measurements, 70 km was specified as the characteristic AF wavelength. Determining the eddy production rate was much more difficult. Direct defining this factor was not possible and only approximated values could be used. The literature does not provide precise information about this value. The rapid production of a single eddy in 3 to 7 days is possible (Johannessen et al., 1987). A similar value, obtained from a two level model, was used in calculations for the Iceland-Faeroes Front (Allen et al., 1994).

Finally, for the purpose of approximating the mean time needed for eddy creation, it was assumed that this time should not be shorter than the time needed for eddy circulation period. 40 days was chosen as the most probable value. Calculations of transfrontal transport across the 800 km long front, with mean parameters of the eddy, produced the following results:

$$Q_Q = 17.7 \times 10^{12}\,\mathrm{W}$$
$$Q_{\mathrm{Sal}} = 188 \times 10^{3}\,\mathrm{kg\,s^{-1}}$$
$$Q_{\mathrm{Vol}} = 2.1\,\mathrm{Sv}$$

The eddy supported heat transport Q_Q which was obtained is two times bigger than the value estimated by van Aken et al. (1995) (8×10^{12} W). The delivered heat Q_Q if released from the Greenland Sea Gyre (surface 1.34×10^{11} m^2) into the atmosphere would produce a heat flux of 132 W m^{-2}. This result is less than the mean annual heat flux from the Greenland Sea to the atmosphere which is 160 W m^{-2} (Hopkins, 1991). Segtnan et al. (2011) calculated that in order to close the Greenland Sea budget, the cross-frontal heat fluxes of 35 TW across the Arctic Front is necessary. They estimate that the volume transport across the whole front dividing the Greenland and Norwegian seas equals 4 Sv.

OSD
10, 985–1030, 2013

5 The eastern border

5.1 Structure

The eastern WSC branch is related to the shelf break and slope and continues over the 800 m isobath (Fig. 1). Border of the Atlantic domain follows east of this flow, over the Barents Sea slope and western Spitsbergen shelf and slope. The AW flow frequently crosses the 800 m isobath, penetrates the trough between the Bear Island and Sørkapp (southern tip of Spitsbergen) – the Storfiordrenna, advects over the shelf and even flows into the western Spitsbergen fiords. The front dividing the Atlantic origin and the Arctic Waters from the Barents Sea was sometimes called the Barents Sea Polar Front (Gawarkiewicz and Pluedemann, 1995). In the Spitsbergen vicinity the shallow water front is often called the Arctic Front (Saloranta and Svendsen, 2001). They state that the coastal front west of Spitsbergen is a part of the Nordic Seas frontal system as a continuation of the front at the Barents Sea (Barents Sea Polar Front). Herein, after Skogseth et al. (2006) and other authors we call the front separating the warm Atlantic origin waters from the cold Arctic waters from the east the "Polar Front".

Between the Bear Island and Sørkapp, the frontal line is complicated because part of the AW circulates cyclonically in the troughs – Storfiordrenna and Kvintehola (Fig. 12). In this region, the Bjørnøya Current maintains the front on the right, shallow water side. West of the Svalbard the shelf waters originate mostly from the East Spitsbergen Current (Saloranta and Svendsen, 2001). On the shelf, the freshwater input from the glaciers and rivers gives an additional contribution (Meredith et al., 2001). The current carrying the cold and less saline waters around the southern Spitsbergen tip is often called the Sørkapp Current or the South Cape Current, whereas the flow over the western Spitsbergen shelf – the Coastal Current.

There is a strong front of properties between the Sørkapp Current and AW in the Storfiordrenna (Fig. 12). At 100 m temperature on both sides of the front varies between −0.2 °C and 6 °C, salinity between 34.67 and 35.13, density between 27.84 kg m^{-3} on the cold side and 27.68 kg m^{-3} on the AW side. It makes the horizontal gradients of

OSD
10, 985–1030, 2013

temperature equal to 0.27 °C km^{-1}, salinity: 0.021 km^{-1} and density: 0,007 kg m^{-3} km^{-1}. Temperature and salinity gradients are stronger than in the AF, but the density gradient is much weaker.

West of Svalbard the front line continues over the shelf edge (Fig. 13). The temperature and salinity horizontal gradients are weaker than in the Sørkapp region, the density gradient vanishes; the salinity and temperature changes compensate each other. Colder, less saline shelf water overlies the AW. There are numerous intrusive structures; AW penetrates over the shelf.

5.2 Dynamics

The WSC is the primary source of heat and salt to the AO, the WSC core and its extension in the Arctic Ocean – the Svalbard branch – plays a major role in this transport. It gives a nearly constant volume flux – the long-term mean of the northward transport is 1.8 ± 0.1 Sv, including 1.3 ± 0.1 Sv of the AW warmer than 2 °C (Beszczynska-Möller et al., 2012).

This flow is a continuation of the eastern branch of the Norwegian Atlantic Current (the Norwegian Atlantic Slope Current), coherent barotropic flow continuing over the western Norway slope. Also in the northern part the current appears as a concentrated, 40 km wide stream. The flow preserves the barotropic type, however, the baroclinic depth-related component is also apparent. At the latitude of 75° N the eastern WSC branch baroclinic currents transports 1.23 Sv of water warmer than 2 °C and saltier than 34.90 and 16 TW of heat (mean for summers 2000–2010). These are values comparable with the volume and heat delivered by the Svalbard branch to the Arctic Ocean, at the latitude of 78°50′ N.

Continuing north, the baroclinic transport decreases (Table 1). It may be caused by the loss of buoyancy by the current. The baroclinic jetstream decreases its transport as the buoyancy is lost from the surface layer. This decrease in transport is compensated by an increase in the barotropic flow on the slope (Walin et al., 2004).

OSD
10, 985–1030, 2013

5.3 The transfrontal exchange

There is a very weak density gradient or no gradient at all between the AW and the shelf/coastal waters on the eastern AD border. Additionally, there is a strong horizontal velocity shear – the core of the AW flows much faster than the shelf waters. This outline suggests that the barotropic instability should be the main mechanism of the current destabilization and crossfrontal exchange. Indeed, Nilsen et al. (2006) write that the Gaussian current profiles for narrower current jets in the WSC core produce unstable modes due to a stronger velocity shear. The unstable eddies probably contribute significantly to the heat loss of the WSC warm core by isopycnal eddy diffusion. Cottier et al. (2005) found that the barotropic instabilities forms pockets of the AW at the shelf front. The AW leaks onto the shelf and propagates as topographically steered features toward the fjords. Cottier et al. (2007) described the warm AW inflow over the shelf in winter 2005/2006 caused by sustained along-shelf winds generating upwelling and crossfrontal exchange.

The tidal forcing is an additional mechanism promoting the cross-shelf exchange. Tides propagate as coastal Kelvin waves along the Spitsbergen coast (Kowalik, 1994). Diurnal tides can be enhanced near the shelf edges causing generation of shelf waves with tidal periods (Nilsen et al., 2006). Kasajima and Svendsen (2002) found increasing of the cross-shelf velocity component of diurnal tides from deep water to the shelf edge.

The ice and brine production is another mechanism of cross-slope exchange. The Storfjorden is the region of the biggest brine production in the Svalbard Archipelago, Storfiordrenna is the pathway of the brines westward transport. Conditions of freezing, brine release and transportation should be the most important here; but also the brine production in smaller West Spitsbergen fiords influence the exchanges mechanisms (Nilsen et al., 2008).

IOPAN investigations of the western Barents Sea and Spitsbergen slope/shelf show a variety of mesoscale structures. There are isopycnal intrusions, pockets of the AW

OSD
10, 985–1030, 2013

separated from the mean flow and advected over the shelf, domes of brines migrating down along the Storfjordrenna slope (Fig. 14).

The shelf is a transition zone between the warm AW and fiords. The western Spitsbergen large fiords systems – Hornsund, Belsund, Isfjorden and Kongsfjorden are influenced by the AW properties change (Walczowski and Piechura, 2011) and deep basin – shelf – fiord exchange (Cottier et al., 2006). Surprisingly, the southernmost Hornsund is much colder and more "Arctic" than the northernmost Kongsfjorden, which is characterized as the Atlantic type. Bottom topography promote easier water exchange in Kongsfjorden. Additionally, Hornsund is isolated from the AW stream by the intensive Sørkapp Current.

6 The fronts variability

Both frontal zones separating the Atlantic origin waters from the Arctic and Polar water masses are related to the bottom topography. The western frontal zone runs meridionally between about 005° E and 006° E, and is "semipermanent" (Van Aken, 1995). Its position is associated with the mid-ocean ridges. The frontal zone bordering the AD from the east is related to the Barents Sea and western Spitsbergen slope and shelf.

Positions of both zones are not permanent, it changes depending of the intensity of the AW flow, frontal instabilities, atmospheric conditions and other processes. In warm years and high activity of the WSC western branch, the AF line moves westward (Fig. 15). Also the mesoscale activity changes the position of the fronts. Processes of the meanders growth and eddies formation may shift the frontal line by tens of kilometres westward (Walczowski and Piechura, 2007). Changes of the AF position and strength may be also affected by winds over the Nordic Seas and the NAO index (Schlichtholtz and Goszczko, 2006). They found the large negative correlation between the NAO index and the AW flow at the latitude of 76°30′ N, in the ridge area.

The core of the WSC seems to be more stable in the southern part than in the northern one. At latitude 75° N, the position of the core (peak of the AW integrated transport

OSD
10, 985–1030, 2013

at the 290th km of section) appears in the same position in several years (Fig. 16 a). At 76°30 N the axis of the current moves zonally by 50 km. It may be caused by the Sørkapp Current activity. Transport peaks of the western branch are also concentrated more at the 75° N parallel than at 76°30 N. Between the two flows maxima, significant mesoscale activity is apparent. The mesoscale eddies occur also west of the AF.

There is large seasonal and interannual variability of the AW properties (Beszczynska-Möller et al., 2012). It concerns both branches of the WSC flow. The AW carried along the western WSC branch is colder and less saline than the AW transported by the WSC core along the shelves (Fig. 17). At the latitude of 76°30′ N, at 200 m, the mean differences for summers 1996–2010 equal 1.75 °C for temperature and 0.062 for salinity. The changes of these properties occur in both branches simultaneously, with positive trends and maximum in 2005–2006 period. The correlation coefficients for data presented at Fig. 17 equalled $r = 0.64$, $p = 0.008$ for temperature and $r = 0.83$, $p = 0.0001$ for salinity, without time lag. For detrended data correlations are smaller, $r = 0.48$, $p = 0.06$ and $r = 0.56$, $p = 0.02$, respectively.

The differences of T and S are due to various origins and pathways of the AW. The western branch is fed by the Faroe branch of the AW inflow, which is about 2 °C colder and less saline than the AW transported through the Faeroe-Shetland Channel (Hansen et al., 1999). The differences could be also caused by the longer residence of water continuing along the AF; the signal propagation velocity in the western branch is lower than that in the eastern one (Walczowski and Piechura, 2007). Therefore, water releases more heat to the atmosphere and mixing processes in the AF cause water cooling, and freshening.

In summers 2005 and 2006 some uncommonly large eddies were observed (Walczowski and Piechura, 2007). These eddies carried unusual amount of heat along the western border of the Atlantic domain. The maximum of the front westward shift at the section along the 76°30′ N parallel during the period 1996–2010 occurred in these warmest 2005 and 2006 yr (Fig. 18). During that time temperature and salinity in both

OSD
10, 985–1030, 2013

WSC branches rose; the 2000 warming was manifested mostly by the core T and S increasing.

7 Front bifurcation

Continuing towards the Fram Strait both AW branches converge (Fig. 19a) due to the bottom topography; the distance between the Knipovich Ridge and the Svalbard shelf break is least at the latitude of 78° N. In the Fram Strait the structure of the AD changes. The West Spitsbergen Current diverges again into two or even three streams. The eastern one – the Svalbard Branch, and the central one – the Yermak Branch, flow into to the Arctic Ocean through the Fram Strait. The Svalbard Branch, fed by the along-slope core of the WSC, after passing the Fram Strait, continues eastward along the shelf break. The local front separates this AW flow from the Barents Sea waters located on the south. Due to significant transformation and densification, the AW in this region usually subducts under the layer of Polar Waters. The water mass configuration gets complicated near the St. Anna Trough where the Svalbard Branch meets the AW Barents Branch (Rudels et al., 2013).

The offshore branch recirculates westward and then southward. The recirculation and the Arctic Front bifurcation is the most intensive between 78° N and 79° N (Fig. 19b). Northward baroclinic stream of the AW carried by this flow vanishes, mesoscale eddies carry the AW westward and southward. Sometimes unusually big heat anomalies from the western branch are able to cross the Fram Strait and inflow the Arctic Ocean (Walczowski and Piechura, 2007). The AW warm water pulses may influence the ice conditions north of Svalbard (Piechura and Walczowski, 2009).

8 Conclusions

Results show that AF baroclinic jet streams are a significant source of the AW and cannot be ignored in the Nordic Sea mass, heat and salt balance. At high latitudes

OSD
10, 985–1030, 2013

baroclinic transport of the AW is comparable or even larger than the volume transport along the shelf break, which is commonly regarded as the main AW stream in the Nordic Seas. The transfrontal transport of the AW occurs along the whole AF. The baroclinic, mesoscale anticyclonic eddies are the main structures carrying the AW into the Greenland Sea. Eddies are created due to the front baroclinic instability, amplified by the bottom topography.

The transfrontal transport and final AF bifurcation is important for the whole Nordic Seas system, especially for maintenance of the thermohaline circulation. The return Intermediate Atlantic Water plays a significant role in the convection and deep water mass formation in the Greenland Sea (van Aken, 2007).

Transport cross the eastern AD border is less intense. The eastern branch (core) of the West Spitsbergen Current preserves its signature on the long way to the Arctic Ocean. The ocean-atmosphere heat exchange is the main process modifying the core water properties. The transfrontal exchange is mostly important for the Svalbard fiords, modifying their physical conditions.

Acknowledgements. The hydrographic data were collected under the European Union Fifth Framework Program project ASOF-N (Arctic-Subarctic Ocean Flux Array for European Climate: North), contract number EVK2-CT-200200139, and the Sixth Framework Program DAMOCLES (Developing Arctic Modeling and Observing Capabilities for Long-term Environment Studies), contract number 018509GOCE. This research was supported by the Polish – Norwegian grant AWAKE, PNRF-22-AI-1/07. The author is grateful to the entire crew of R/V *Oceania* and the colleagues who participated in the work at sea.

References

Aagaard, K. and Carmack, E.: The role of sea ice and other fresh water in the arctic circulation, J. Geophys. Res., 94, 14485–14498, 1989.

Allen, J. T., Smeed, D. A., and Chadwick, A. L.: Eddies and mixing in the Iceland-Faeroes Front, Deep-Sea Res., 41, 51–79, 1994.

OSD

10, 985–1030, 2013

Beszczynska-Möller, A., Fahrbach, E., Schauer, U., and Hansen, E.: Variability in Atlantic water temperature and transport at the entrance to the Arctic Ocean, 1997–2010, ICES J. Mar. Sci., 69, 852–863, doi:10.1093/icesjms/fss056, 2012.

Cisewski, B., Budeus, G., and Krause, G.: Absolute transport estimates of total and individual water masses in the northern Greenland Sea derived from hydrographic and acoustic Doppler current profiler measurements, J. Geophys. Res., 108, 3298, doi:10.1029/2002JC001530, 2003.

Cottier, F., Tverberg, V., Inall, M., Svendsen, H., Nilsen, F., and Griffiths, C.: Water mass modification in an Arctic fjord through cross-shelf exchange: the seasonal hydrography of Kongsfjorden, Svalbard, J. Geophys. Res., 110, C12005, doi:10.1029/2004JC002757, 2005.

Cottier, F. R., Nilsen, F., Inall, M. E., Gerland, S., Tverberg, V., and Svendsen, H.: Wintertime warming of an Arctic shelf in response to large-scale atmospheric circulation, Geophys. Res. Lett., 34, L10607, doi:10.1029/2007GL029948, 2007.

Dietrich, G., Kalle, K., Krauss, W., and Siedler, G.: General Oceanography, 2nd Edn., Wiley-Intersci., New York, 626, 1980.

Dixon, R., Maincke, J., Rhines, P.: Arctic-Subarctic ocean fluxes: defining the role of the Northern Seas in climate, in: Arctic-Subarctic Ocean Fluxes, Springer Science, 1–15, 2008.

Druet, C.: Dynamika Stratyfikowanego Oceanu, PWN Warszawa, 146 pp., 1994.

Druet, C.: Elementy Hydrodynamiki Geofizycznej, PWN Warszawa, 111 pp., 1995.

Emery, W. J. and Thomson, R. E.: Data analysis methods in physical oceanography, Elsevier, Amsterdam, 650, 2001.

Fedorov, K. N.: The Physical Nature and Structure of Oceanic Fronts, Springer-Verlag, New York, 333 pp., 1986.

Furevik, T.: On anomalous sea surface temperatures in the Nordic Seas, J. Climate,13, 104–1053, 2000.

Gawarkiewicz, G. and Pluedemann, A. J.: Topographic control of the thermohaline frontal structure in the Barents Sea Polar Front on the south flank of the Spitsbergen Bank, J. Geophys. Res., 100, 4509–4524, 1995.

Hallock, Z. R.: Variability of frontal structure in the Southern Norwegian Sea, J. Phys. Oceanogr., 15, 1245–1254, 1985.

Hansen, B. and Østerhus, S.: North-Atlantic-Nordic Seas exchanges, Prog. Oceanogr., 45, 109–208, 2000.

OSD
10, 985–1030, 2013

Hansen, B., Larsen, K. M. H., Østerhus, S., Turrell, B., and Jónsson, S.: The Atlantic Water inflow to the Nordic Seas, The International WOCE Newsletter, 35, 33–35, 1999.
Hopkins, T. S.: The GIN Sea-A synthesis of its physical oceanography and literature review 1972–1985, Earth-Sci. Rev., 30, 75–318, 1991.
Ivanov, V. and Korablev, A.: Structure and dynamic of hydrological fronts, in Large-scale processes in Norway Energetic Zone and adjacent regions, Gidrometeoizdat, Sankt-Petersburg, 41–55, 1994 (in Russian).
Johannessen, O. M.: Brief overview of the physical oceanography, in: Nordic Seas, edited by: Hurdle, B. G., 103–127, Springer, New York, 1986.
Johannessen, J. A., Johannessen, O. M., Svendsen, E., Shuchman, R., Mendley, T., Campbell, W. J., Josberger, E. G., Sandven, S., Gascard, J.-C., Olaussen, T., Davidson, K., and van Leer, J.: Meso-scale eddies in the Fram Strait marginal ice zone during the 1983 and 1984 marginal ice zone experiments, J. Geophys. Res., 92, 6754–6772, 1987.
Kasajima, Y. and Svendsen, H.: Tidal features in the Fram Strait, Cont. Shelf Res., 22, 2461–2477, 2002.
Kowalik, Z.: Modeling of topographically amplified diurnal tides in the Nordic Seas, J. Phys. Oceanogr., 24, 171–1731, 1994.
Kuhlbrodt, T., A. Griesel, M., Montoya, A., Levermann, M., Hofmann, and Rahmstorf, S.: On the driving processes of the Atlantic meridional overturning circulation, Rev. Geophys., 45, RG2001, doi:10.1029/2004RG000166, 2007.
Latarius, K. and Quadfasel, D.: Seasonal to interannual variability of temperature and salinity in the Greenland Sea: heat and freshwater budgets, Tellus A, 62, 497–515, 2010.
Maslowski, W., Marble, D., Walczowski, W., Schauer, U., Clement, J. L., and Semtner, A. J.: On climatological mass, heat, and salt transports through the Barents Sea and Fram Strait from a pan-Arctic coupled ice-ocean model simulation, J. Geophys. Res., 109, C03032, doi:10.1029/2001JC001039, 2004.
Mauritzen, C., Hansen, E., Andersson, M., Berx, B., Beszczynska-Möller, A., Burud, I., Christensen, K. H., Debernard, J., de Steur, L., Dodd, P., Gerland, S., Godøy, Ø., Hansen, B., Hudson, S., Høydalsvik, F., Ingvaldsen, R., Isachsen, P. E., Kasajima, Y., Koszalka, I., Kovacs, K. M., Køltzow, M., LaCasce, J., Lee, C. M., Lavergne, T., Lydersen, C., Nicolaus, M., Nilsen, F., Nøst, O. A., Orvik, K. A., Reigstad, M., Schyberg, H., Seuthe, L., Skagseth, Ø., Skarðhamar, J., Skogseth, R., Sperrevik, A., Svensen, C., Søiland, H., Teigen, S. H., Tverberg, V., and Wexels Riser, C.: Closing the loop – approaches to monitoring the state of the

OSD
10, 985–1030, 2013

Arctic Mediterranean during the International Polar Year 2007–2008, Prog. Oceanogr, 90, 62–89, doi:10.1016/j.pocean.2011.02.010, 2011.
Meredith, M., Heywood, K. J., Dennis, P., Goldson, L., White, R., Fahrbach, E., Schauer, U., and Østerhus, S.: Freshwater fluxes through the western Fram Strait, Geophys. Res. Lett., 28, 1615–1618, 2001.
Nilsen, F., Gjevik, B., and Schauer, U.: Cooling of the West Spitsbergen Current: isopycnal diffusion by topographic vorticity waves, J. Geophys. Res., 111, C08012, doi:10.1029/2005JC002991, 2006.
Nilsen, F., Cottier, F., Skogseth, R., and Mattsson, S.: Fjord – shelf exchanges controlled by ice and brine production: the interannual variation of Atlantic Water in Isfjorden, Svalbard, Cont. Shelf. Res., 28, 1838–1853, 2008.
Orvik, K. A. and Niiler, P.: Major pathways of Atlantic water in the northern North Atlantic and the Nordic Seas toward the Arctic, Geophys. Res. Lett., 29, 1896, L015002, doi:10.1029/2002GL015002, 2002.
Orvik, K. A. and Skagseth Ø.: The impact of the wind stress curl in the North Atlantic on the Atlantic inflow to the Norwegian Sea toward the Arctic, Geophys. Res. Lett., 30, 1884, doi:10.1029/2003GL017932, 2003.
Osiński, R., Wieczorek, P., Beszczynska-Moller, A., and Goszczko, I.: ADCP-referenced geostrophic veqlocity and transport in the West Spitsbergen Current, Oceanologia, 45, 425–435, 2003.
Piechura, J. and Walczowski, W.: The Arctic Front: structure and dynamics, Oceanologia, 37, 47–73, 1995.
Piechura, J. and Walczowski, W.: Warming of the West Spitsbergen Current and sea ice north of Svalbard, Oceanologia, 51, 147–164, 2009.
Rudels, B., Schauer, U., Björk, G., Korhonen, M., Pisarev, S., Rabe, B., and Wisotzki, A.: Observations of water masses and circulation with focus on the Eurasian Basin of the Arctic Ocean from the 1990s to the late 2000s, Ocean Sci., 9, 147–169, doi:10.5194/os-9-147-2013, 2013.
Segtnan, O. H., Furevik, T., and Jenkins, A. D.: Heat and freshwater budgets of the Nordic seas computed from atmospheric reanalysis and ocean observations, J. Geophys. Res., 116, C11003, doi:10.1029/2011JC006939, 2011.
Schauer, U., Loeng, H., Rudels, B., Ozhigin, V., and Dieck, W.: Atlantic water flow through the Barents and Kara Sea, Deep-Sea Res. Pt. I, 49, 2281–2296, 2002.

OSD
10, 985–1030, 2013

Schlichtholz, P. and Goszczko, I.: Interannual variability of the Atlantic water layer in the West Spitsbergen Current at 76.5° N in summer 1991–2003, Deep-Sea Res. Pt. I, 53, 608–626, doi:10.1016/j.dsr.2006.01.001, 2006.
Skogseth, R., Sandvik, A. D., and Asplin, L.: Wind and tidal forcing on the meso-scale circulation in Storfjorde n, Svalbard. Cont. Shelf. Res., 27, 208–227, doi:10.1016/j.csr.2006.10.001, 2006.
Saloranta, T. M. and Svendsen, H.: Across the Arctic front west of Spitsbergen: high-resolution CTD sections from 1998–2000, Polar Res., 20, 17–184, 2001.
Spall, M. A.: Baroclinic Jets in Confluent Flow, J. Phys. Oceanogr., 27, 1054–1071, 1997.
Swift, J. H.: The Arctic waters, in: The Nordic Seas, edited by: Hurdle, B. G., Springer-Verlag, New York, 124–153, 1986.
Thurnherr, A. M., How To Process LADCP Data With the LDEO Software, available at: ftp://ftp.ldeo.columbia.edu/pub, (last access: 2008), 2007.
Van Aken, H. M.: The Oceanic Thermohaline Circulation: an Introduction, Springer Science+Business Media, LLC, ISBN-10: 0-387-36637-7, 2007.
Van Aken, H. M., Budeus, G., and Hähnel, M.: The anatomy of the Arctic Frontal Zone in the Greenland Sea, J. Geophys. Res., 100, 15999–16014, 1995.
Walczowski, W.: Transfrontal heat and mass exchange in the Arctic Front region, Ph. D. thesis, 123 pp., Institute of Oceanology PAS, Sopot, 1997.
Walczowski, W. and Piechura, J.: New evidence of warming propagating toward the Arctic Ocean, Geophys. Res. Lett., 33, L12601, doi:10.1029/2006GL025872, 2006.
Walczowski, W. and Piechura, J.: Pathways of the Greenland Sea warming, Geophys. Res. Lett., 34, L10608, doi:10.1029/2007GL029974, 2007.
Walczowski, W. and Piechura, J.: Influence of the West Spitsbergen Current on the local climate, Int. J. Climatol., 31, 1088–1093, doi:10.1002/joc.2338, 2011.
Walczowski, W., Piechura, J., Osinski, R., Wieczorek, P., The West Spitsbergen Current volume and heat transport from synoptic observations in summer (2005), Deep-Sea Res. Pt. I, 52, 1374–1391, doi:10.1016/j.dsr.2005.03.009, 2005.
Walin, G., Broström, G., Nilsson, J., and Dahl, O.: Baroclinic boundary currents with downstream decreasing buoyancy: a study of an idealized Nordic Seas system, J. Mar. Res., 62, 51–543, 2004.

OSD
10, 985–1030, 2013

Table 1. Mean properties of AW ($T > 2\,^{\circ}C$, $S > 34.90$) and baroclinic transports cross the WSC core at sections K and N. Mean for summers 2000–2010, R/V *Oceania* data.

Section	Latitude	Longitude	AW Temp (°C)/Sd	AW Sal/Sd	AW_Vol (Sv)/Sd	Q_Vol (TW)/Sd
K	75°00′ N	13°45′–15°45′ E	4.35/0.31	35.08/0.02	1.23/0.80	16.06/9.68
N	76°30′ N	12°00′–14°00′ E	4.07/0.30	35.07/0.02	0.91/0.56	10.55/6.32

OSD
10, 985–1030, 2013

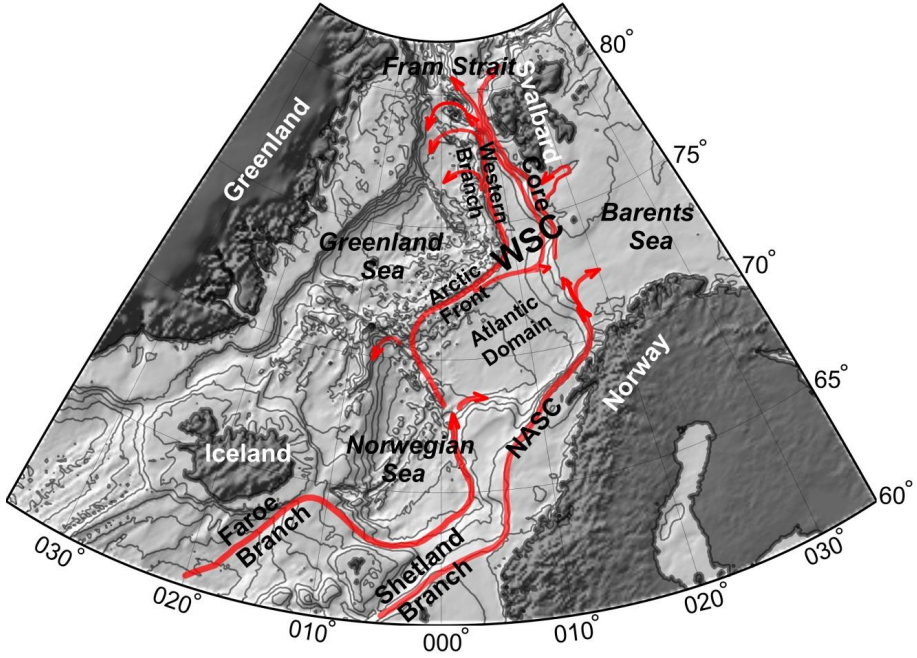

Fig. 1. Nordic Seas bottom topography and Norwegian Atlantic Current – West Spitsbergen Current system.

OSD
10, 985–1030, 2013

Frontal structures in the West Spitsbergen Current margins

W. Walczowski

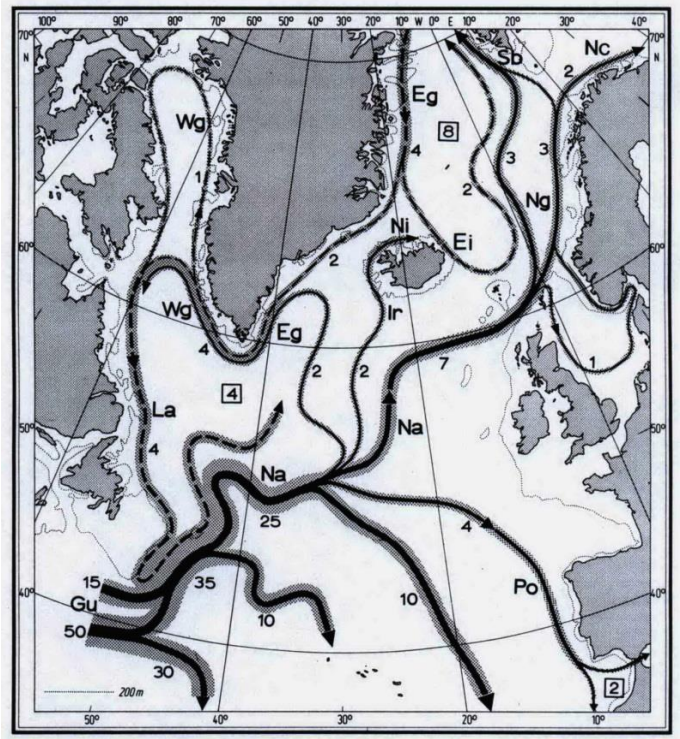

Fig. 2. Scheme of water transport (in $10^6\,m^3\,s^{-1}$) in the layer 0–1000 m in the northern North Atlantic Ocean. (Derived from Wegner, 1973). After Dietrich et al. (1980).

OSD
10, 985–1030, 2013




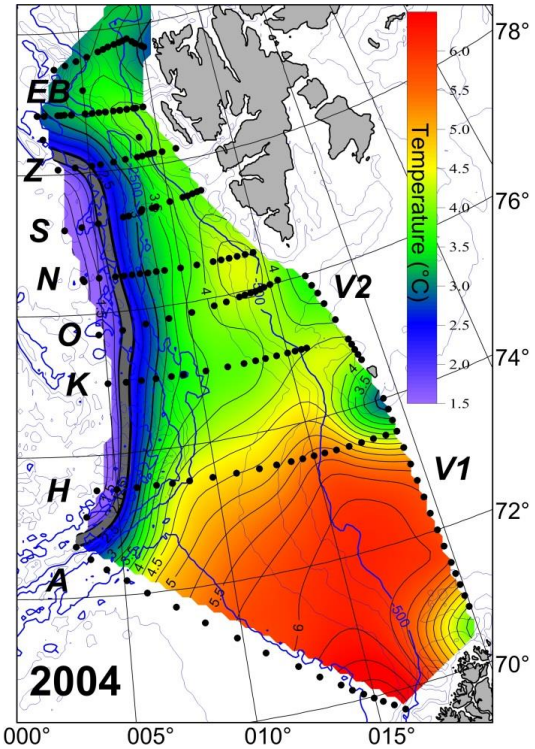

Fig. 3. Temperature at the 200 m level. Positions of the CTD profiles and section names are marked. The Arctic Front position is marked by the grey line.

OSD
10, 985–1030, 2013

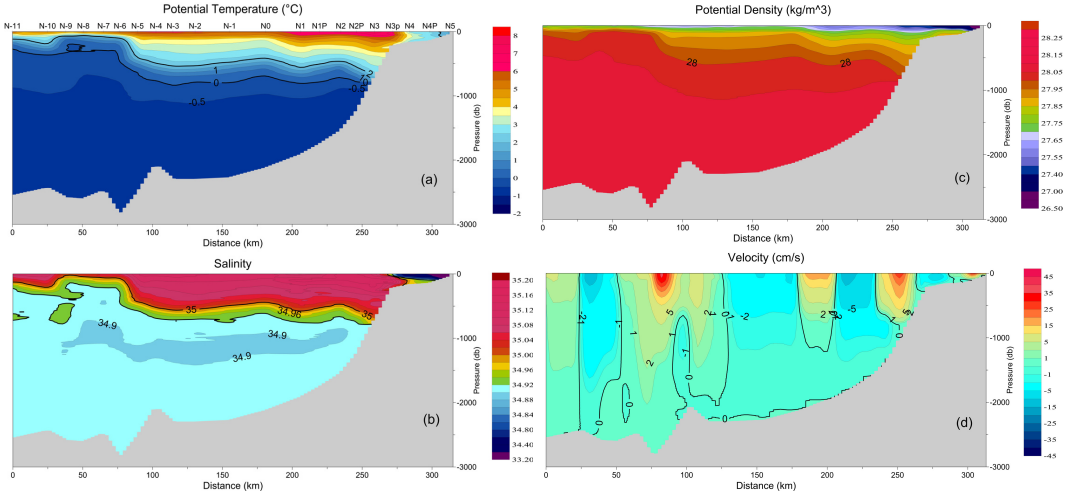

Fig. 4. Section cross the Atlantic domain, along the latitude 76°30′ N, between meridians 4° E and 17° E. **(a)** Potential temperature, **(b)** salinity, **(c)** potential density and **(d)** baroclinic currents fields in summer 2009. 200 m thick layer of the Return AW west of the AF is visible.

OSD
10, 985–1030, 2013

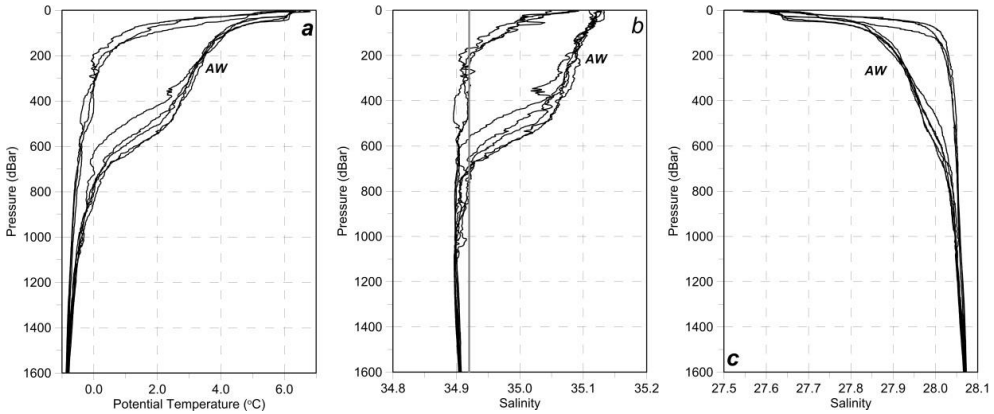

Fig. 5. Profiles of **(a)** temperature, **(b)** salinity and **(c)** density from the both sides of AF. Summer 2009, section "N". Atlantic Water has been indicated by "AW". A vertical line indicating S = 34.92 has been added in the salinity scale.

OSD
10, 985–1030, 2013

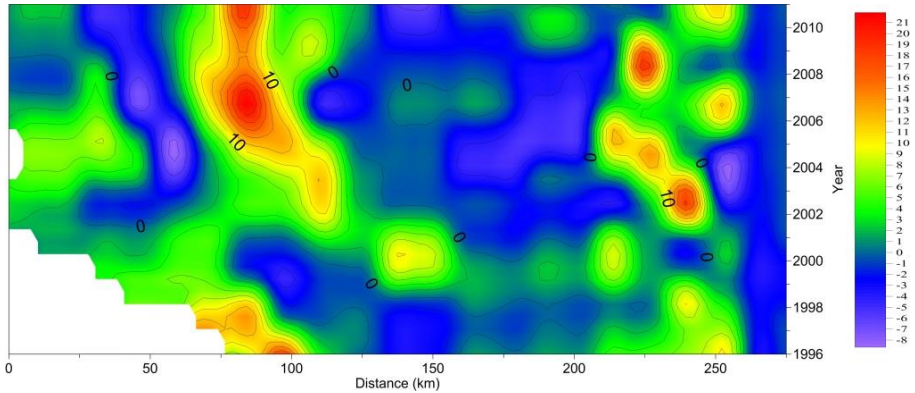

Fig. 6. Section "N" along the 76°30′ N. Hovmoeller diagram of the baroclinic velocity at 200 dbar. Positive values indicate the northward flow.

OSD
10, 985–1030, 2013

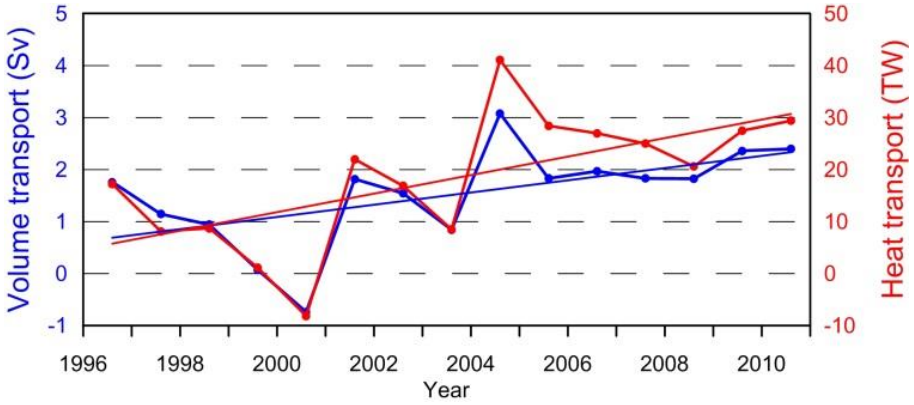

Fig. 7. The geostrophic AW volume and heat transport in summer, at latitude 76°30′ N for the 65 km wide zone between latitudes 6°30′ E and 9° E. R/V *Oceania* data.

OSD
10, 985–1030, 2013

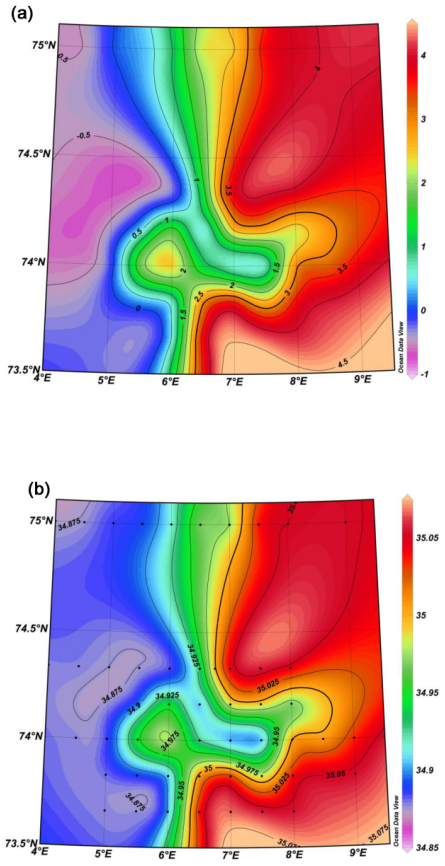

Fig. 8. Summer 1995. **(a)** Temperature and **(b)** salinity at 200 dbar.

OSD
10, 985–1030, 2013

Frontal structures in the West Spitsbergen Current margins

W. Walczowski

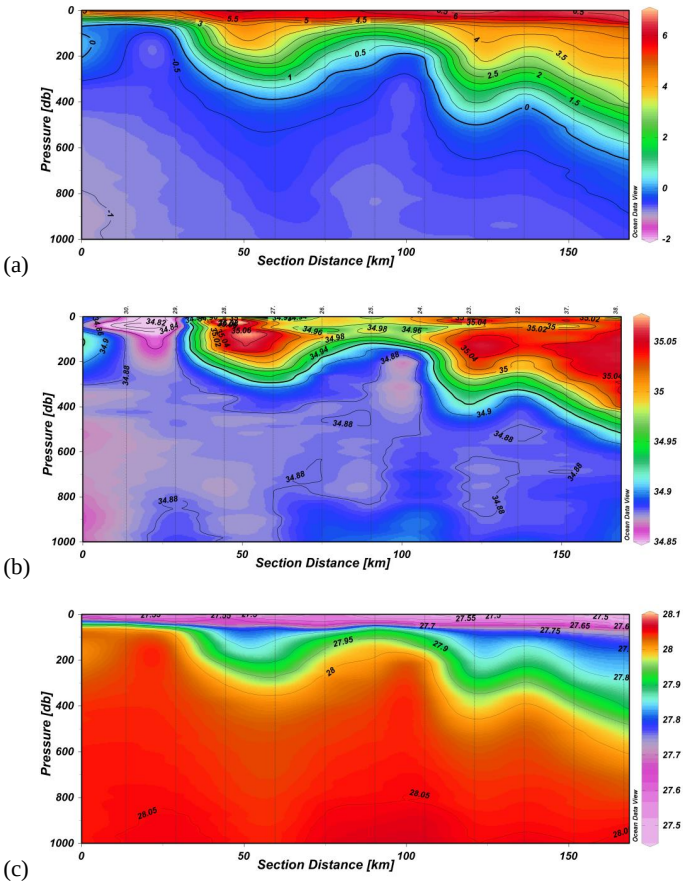

Fig. 9. Section along the 74° N parallel, across the frontal meander and eddy. **(a)** Temperature, **(b)** salinity, and **(c)** potential density.

OSD
10, 985–1030, 2013

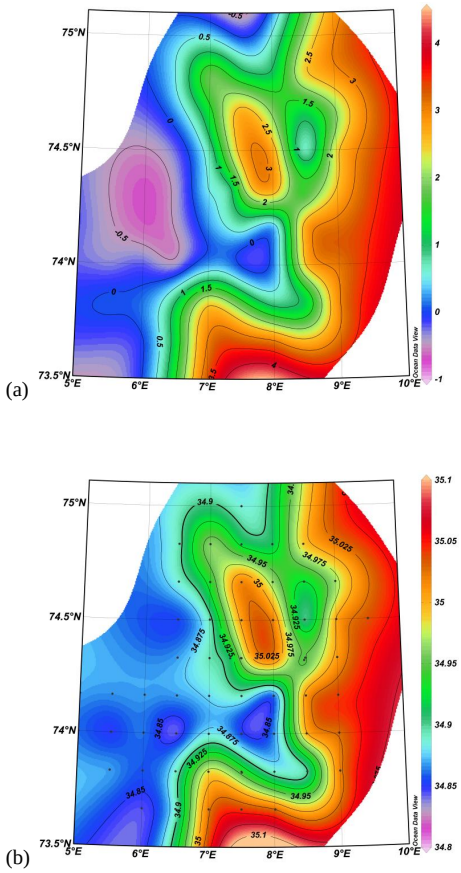

Fig. 10. Summer 1996. **(a)** Temperature and **(b)** salinity at 200 dbar.

OSD
10, 985–1030, 2013

Frontal structures in the West Spitsbergen Current margins

W. Walczowski

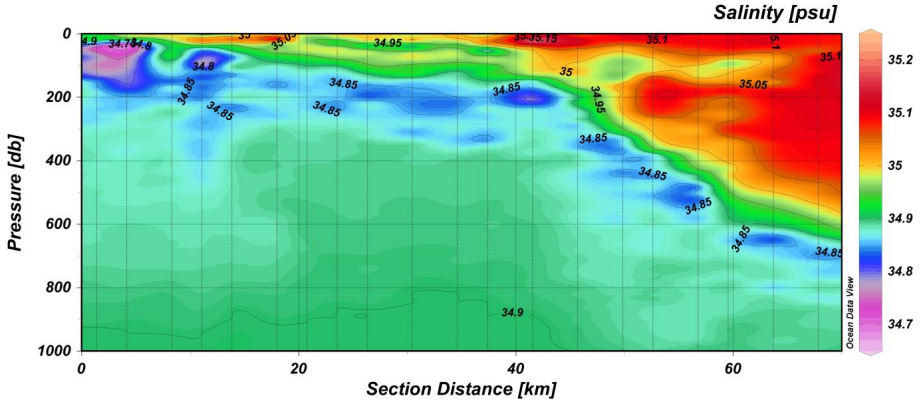

Fig. 11. Low-salinity intrusion of the Arctic water towards the Atlantic domain.

OSD
10, 985–1030, 2013

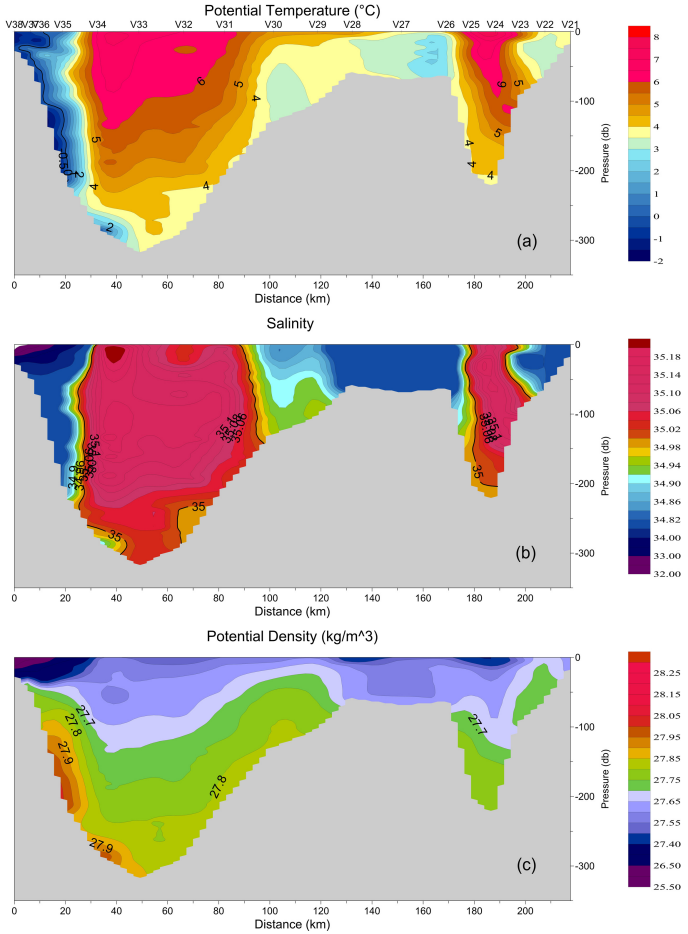

Fig. 12. Section from the Sørkapp at the left hand side to Bear Island. **(a)** Temperature, **(b)** salinity, and **(c)** potential density. Section V2, R/V *Oceania*, summer 2006.

OSD
10, 985–1030, 2013

Frontal structures in the West Spitsbergen Current margins

W. Walczowski

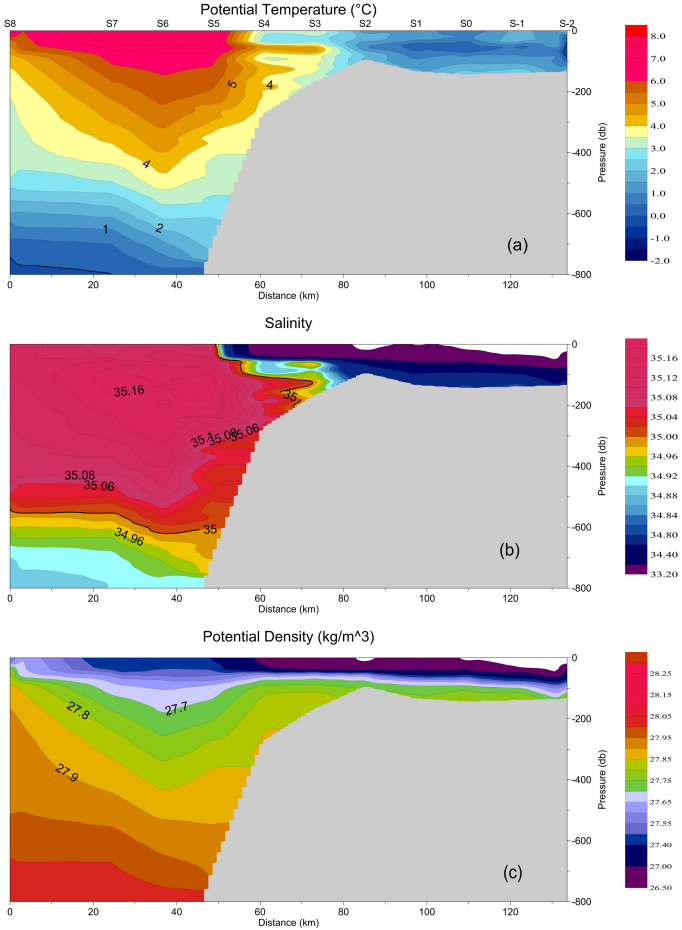

Fig. 13. Section across the core of the WSC and the Polar Front over western Spitsbergen shelf. **(a)** Temperature, **(b)** salinity, and **(c)** potential density. Section "S", R/V *Oceania*, summer 2005.

OSD
10, 985–1030, 2013

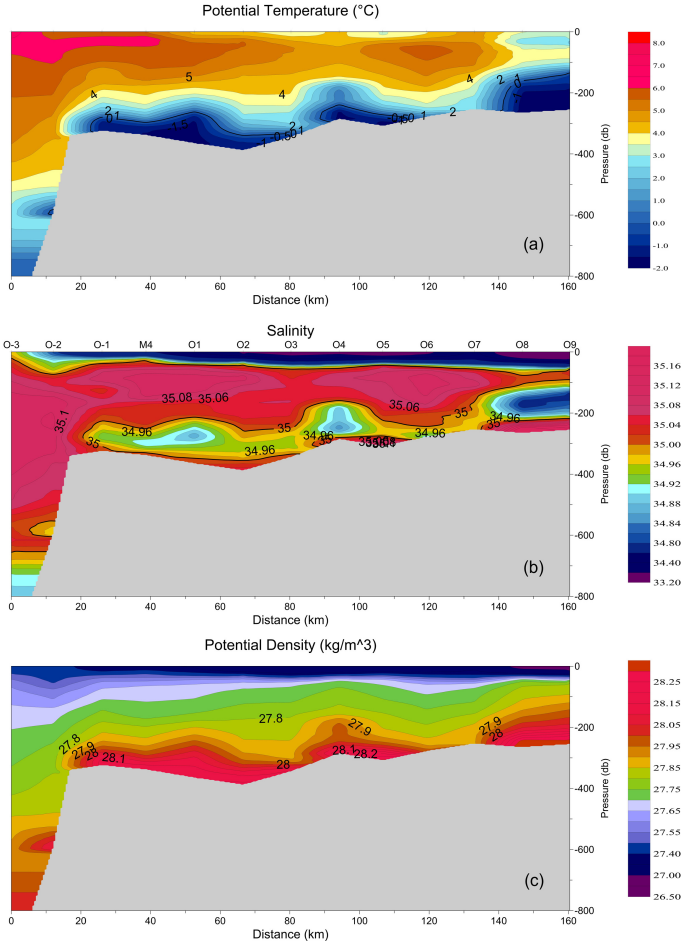

Fig. 14. Inflow of the AW in the upper layer and brines migrating along the Storfiordrenna near the bottom. **(a)** Temperature, **(b)** salinity, and **(c)** potential density. R/V *Oceania*, summer 2000.

OSD
10, 985–1030, 2013

Frontal structures in the West Spitsbergen Current margins

W. Walczowski

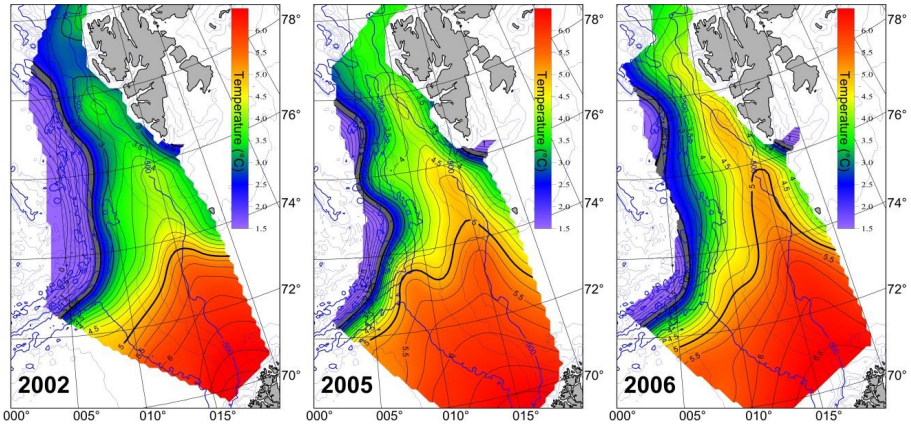

Fig. 15. Temperature at 200 dbar in the cold 2002, and warm 2005, 2006. The western frontal line – isotherms 2–2.25 °C – is marked by the grey line.

OSD
10, 985–1030, 2013

Frontal structures in the West Spitsbergen Current margins

W. Walczowski

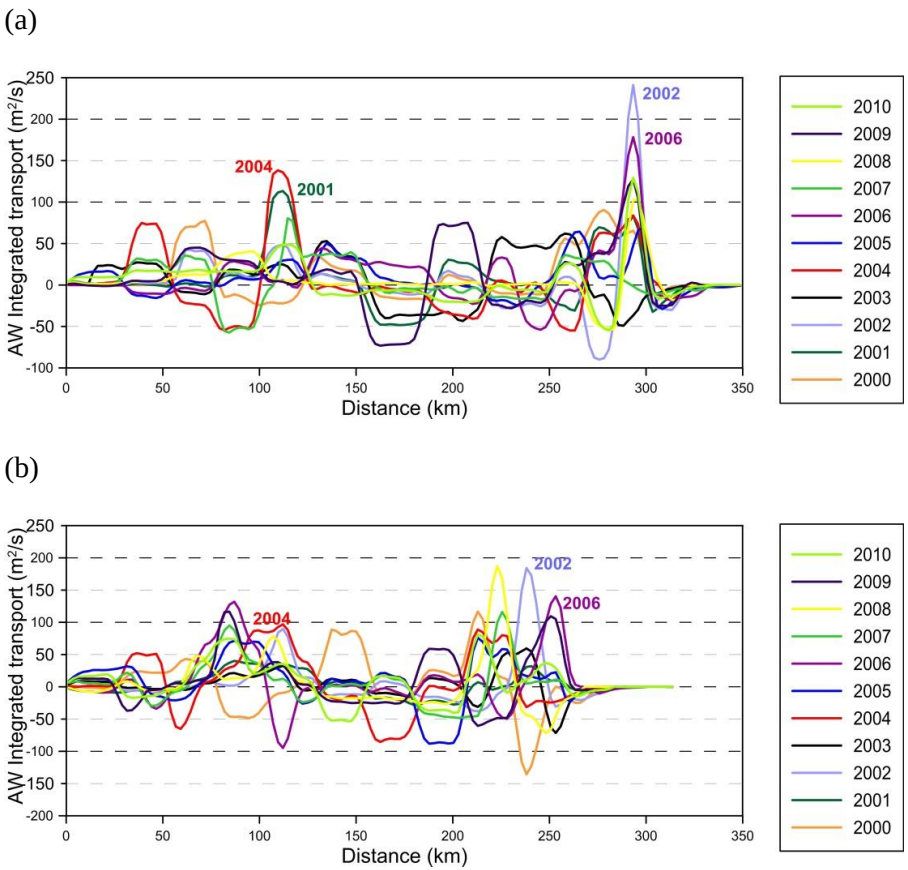

Fig. 16. Vertically integrated baroclinic volume transport ($m^2 s^{-1}$) cross the section **(a)** "K" along the 75° N parallel and **(b)** "N" along the 76°30′ N parallel.

OSD
10, 985–1030, 2013

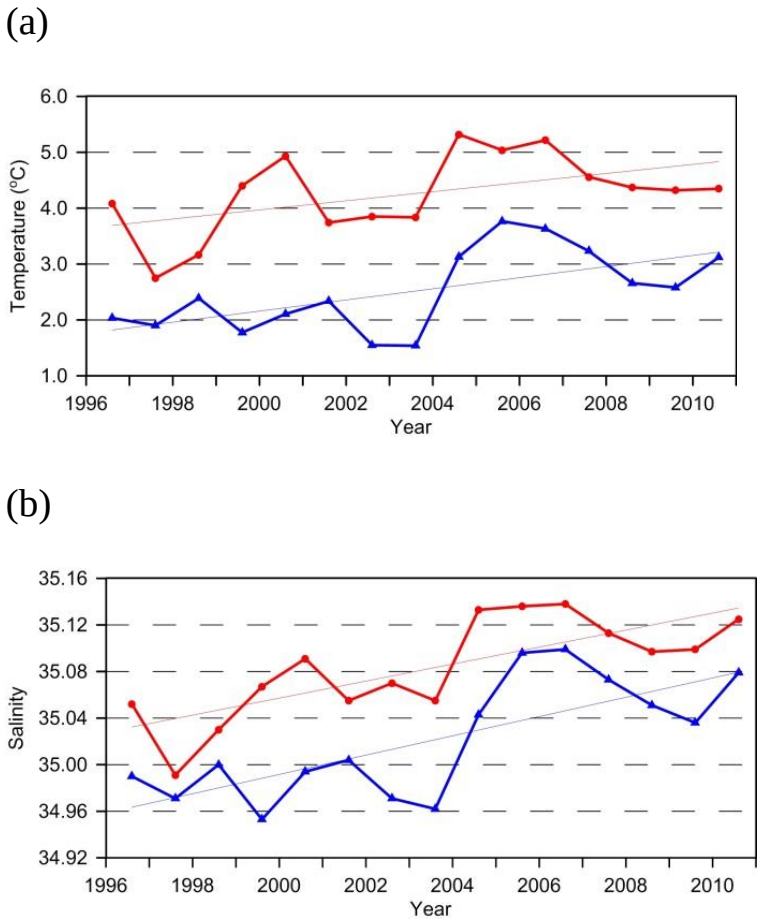

Fig. 17. Time series of mean **(a)** temperature and **(b)** salinity at 200 m depth, in 50 km wide zones of the eastern (red lines) and western WSC branches. AW characterisation: $T > 0$, $S > 34.92$.

OSD
10, 985–1030, 2013

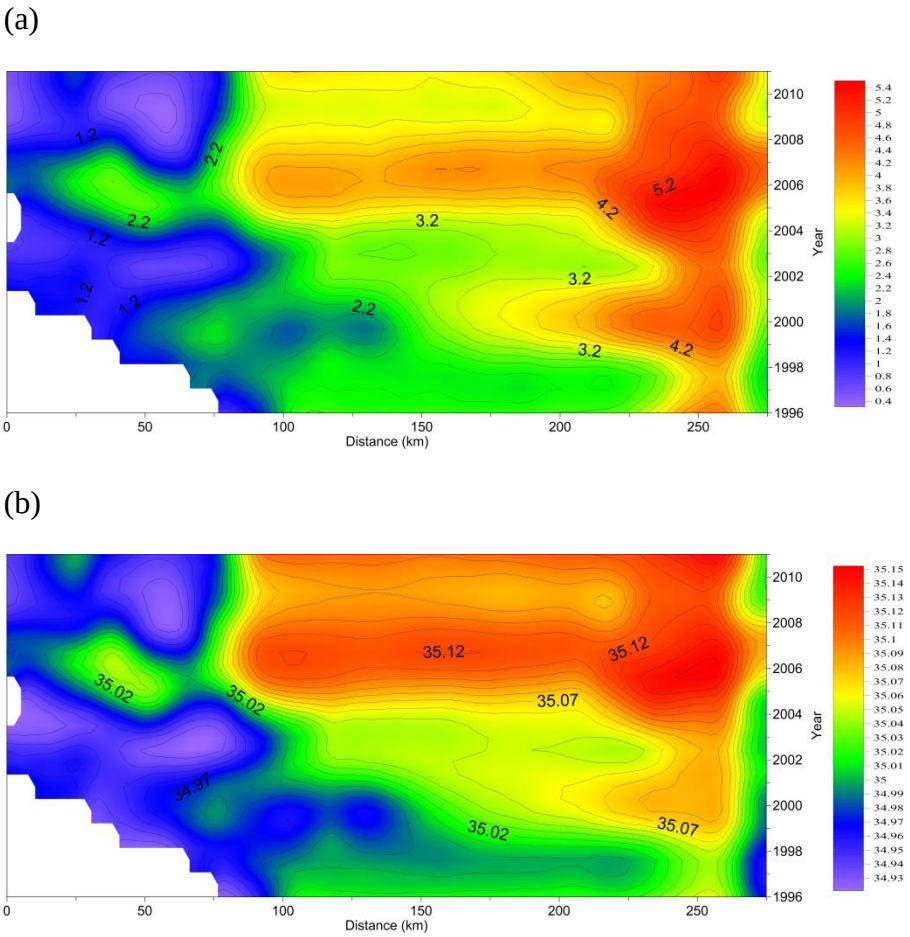

Fig. 18. Section "N" along the 76°30′ N. Hovmoeller diagram of the **(a)** temperature and **(b)** salinity at 200 dbar.

OSD
10, 985–1030, 2013

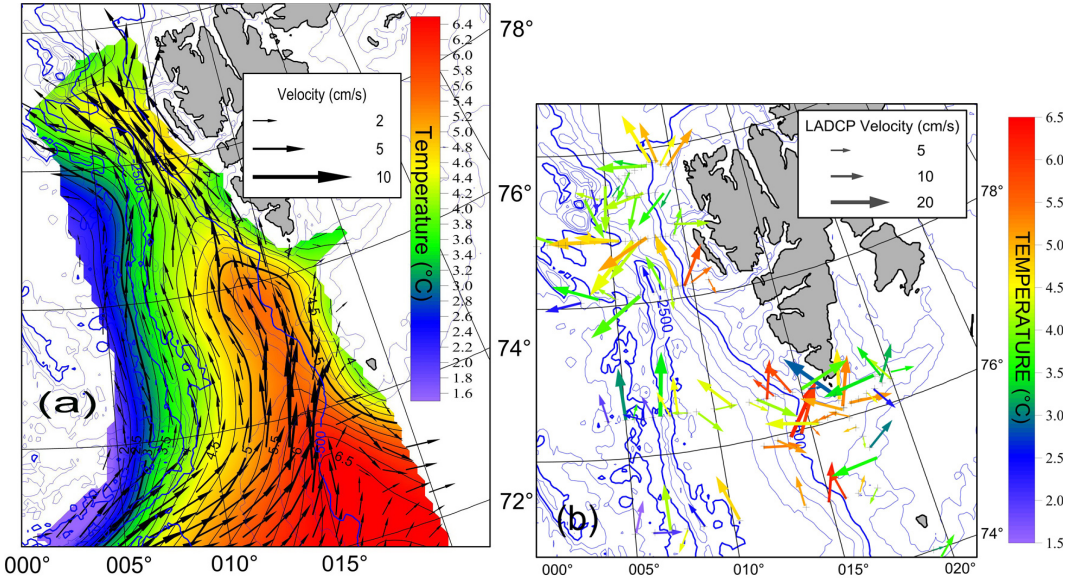

Fig. 19. Summer 2007. **(a)** Baroclinic currents and temperature at 100 dbar and **(b)** LADCP measured currents at 200 dbar.

OSD
10, 985–1030, 2013

Frontal structures in the West Spitsbergen Current margins

W. Walczowski